IOSR Journal of Applied Chemistry (IOSR-JAC)
e-ISSN: 2278-5736.Volume 14, Issue 5 Ser. I (May 2021), PP 05-14
www.iosrjournals.org

Complex formation and aggregation behavior of Congo red in aqueous solution in the presence of gold ions and gold nanoparticles

Moosa AlHoda[1], Jalal Abdulmonem Almeer[1], Hasan Alaudeen Alomari[1], Sultan Akhtar[2], Fryad Z. Henari[1], G. Roshan Deen[1]*

[1] *Biosciences Laboratory, School of Medicine, Royal College of Surgeons in Ireland (RCSI), Medical University of Bahrain, Kingdom of Bahrain.*

[2] *Department of Biophysics, Institute for Research and Medical Consultations (IRMC), Imam Abdulrahman Bin Faisal University, P.O. Box 1982, Dammam 31441, Saudi Arabia*

** Corresponding author (G.R. Deen, Email: rdeen@rcsi.com)*

Abstract

The purpose of this study was to investigate the interaction of a model anionic azo dye Congo red (CR) with gold ions and gold nanoparticles in aqueous solution at 23 ℃ using UV-Vis absorption spectroscopy. The gold nanoparticles were synthesized by a green method using an aqueous extract of cinnamon (Cinnamomom cassia). The cocktail of chemicals (cinnamaldehyde and linalool) in the extract chemically reduced the gold ions to gold nanoparticles and imparted stability to the formed nanoparticles against agglomeration. The synthesized AuNPs were characterized using UV–Vis spectroscopy and Transmission Electron Microscopy (TEM). UV-Vis spectrum shows the Surface Plasmon Resonance (SPR) peak around 536nm. TEM shows the spherical shape of AuNPs and the particle size distribution at around 35 nm with a polydispersity of 15 %.For a fixed concentration of CR (8.78×10^{-5} M) in water containing various concentrations of gold ions, the absorbance peak of CR decreased by 56% ± 6%. This significant decrease in absorbance peak along with the appearance of a broad shoulder at a wavelength of λ = 627 nm indicated the formation of a soluble complex between CR and gold ions. The kinetics of the complex formation between gold ions and CR was found to be a gradual process. Gold nanoparticles at low and high concentrations formed a stable complex with CR. The stability of the complex is attributed to strong electrostatic interactions between CR and gold nanoparticles in solution through the sulfonic groups (SO_3^-) of the dye and the positively charged surface of the nanoparticles. The gold ions and gold nanoparticles under the experimental conditions did not lead to the degradation of dye instead to the formation of stable and unstable complexes, respectively.

Keywords: *Green synthesis, Gold nanoparticle, Congo red, catalytic degradation of dye.*

Article Highlights

- *Green synthesis of stable gold nanoparticles using the extract of cinnamon barks.*
- *Demonstrating the formation of soluble complexes between Congo red and gold ions.*
- *Highlighting the role of chemical reducing agents in catalysis.*

Date of Submission: 03-05-2021 Date of Acceptance: 17-05-2021

I. Introduction

Toxic organic dyes are widely used in textile, leather-tanning, metal-plating, and paper industries. The waste discharge from these industries contains a wide variety of toxic substances such as dyes, heavy metals, and organic solvents. These materials when present above the tolerance level has detrimental effects on living organisms and the ecosystem [1]. Even at low concentrations, the organic dyes cause coloration of water and changes in pH, thus affecting water quality. In human health, the organic dyes cause severe dysfunctions of the reproductive system, kidneys, brain, and the central nervous system [2-6].

In many countries, very strict laws are in place for the removal of organic dyes from industrial effluent before being discharged on land and in water bodies. It must be pointed out, that it is nearly impossible to remove all the dyes present in the effluent, and the discharge contains a very small concentration of the dyes. This has led to a continuous search for new materials and the development of various technologies for the satisfactory removal of dyes from industrial wastewater before the safe discharge [7-10]. A wide range of

methods such as biological treatments, flocculation and coagulation, advanced oxidation and adsorption processes have been widely studied for the removal of a variety of toxic organic dyes from wastewater [11-15].

In recent years, nanoparticles of noble metals such as gold, silver, platinum, and palladium have been widely used for the removal of toxic organic dyes from solution through catalytic processes [16-19]. Among these, gold nanoparticles (AuNPs) have attracted immense biomedical and technological attention due to their catalytic, magnetic, optical, electrical, and anti-microbial properties [20-21]. Gold nanoparticles synthesized by various chemical routes and green methods have been studied for the catalytic reduction of Congo red (CR) dye in aqueous solution [22-25].

Although the catalytic degradation of CR in the presence of metal nanoparticles and a reducing agent has been widely studied, to the best of our knowledge the study of CR interaction with gold ions and gold nanoparticles in the absence of a chemical reducing agent such as sodium borohydride is not widely reported [16-26]. The gold nanoparticles in this study were synthesized by a green method using cinnamon (*Cinnamomom cassia*). Cinnamon extract contains a combination of reducing and stabilizing agents that can be utilized for the synthesis of biocompatible gold nanoparticles from precursor gold salts [27].

The phytochemical composition of cinnamon includes essential oil (1-4%), polyphenols (5-10%), carbohydrates (80-90%), and others such as calcium monoterpene oxalate, resin, mucilage, and gum [27,28]. The essential oil primarily contains primary aldehydes (60-80%) including cinnamaldehyde. The phytochemicals of cinnamon contain functional groups such as aldehyde (–CHO), and hydroxyl units (–OH) in combination with carbohydrates. These functional groups provide synergistic chemical reduction capacity for the reduction of gold salt to gold nanoparticles and their stabilization in a single-step reaction. Further, the nanoparticles produced by this method are non-toxic and have potential applications in pharmacy and nanomedicine [29].

The present study reports on the one-step synthesis of biocompatible gold nanoparticles using the Cinnamon barks as a reducing and a capping agent. The UV-visible absorption spectroscopy and TEM were used to characterize the gold nanoparticles. The synthesised gold nanoparticles exhibit a SPR at 535 nm, with an average size of 35nm.The interaction of gold ions (Au^{3+}) and Au nanoparticles with CR were studied in detail using UV-Vis absorption spectroscopy. The absorption peak of CR reduced in intensity as the concentration of gold salt ($HAuCl_4$) and gold nanoparticles increased. It was demonstrated that the reduction in absorption peak of CR dye by gold ions (Au^{3+}) and gold nanoparticles was mainly the result of formation of a dye-gold ions and dye-gold nanoparticles complexes, respectively. According to our knowledge, the interaction of gold ions (Au^{3+}) and gold nanoparticles (AuNPs) with the anionic dye Cong red in the absence of $NaBH_4$ has not been reported previously.

II. Materials and Methods

2.1 Materials

Cinnamon barks (purchased from the local grocery store), Congo red (Aldrich), and Tetrachloroauric acid ($HAuCl_4$, Aldrich) were used as received. Milli-Q water collected from Milli-Q system (Elix Technology) with a conductivity of 18.2 MΩ cm^{-1} was used for all sample preparations.

2.2 Synthesis of gold nanoparticles

Gold nanoparticles were synthesized using a green method in which an extract of cinnamon from cinnamon barks (*Cinnamomom cassia*) was used as the chemical reducing agent.

Cinnamon barks obtained from a local grocer were washed and rinsed with water (Milli-Q water) and air-dried. The dried barks were ground to a fine powder using a high-duty blender. The cinnamon extract was prepared by adding about 2.50 g of the freshly prepared powder to 100 ml of water in a 250 ml glass beaker. The content was boiled for 5 min under vigorous magnetic stirring and filtered twice using Whatman filter paper (No. 1).

A 1.00 mM aqueous solution of Tetrachloroauric acid ($HAuCl_4$) was prepared by dissolving 0.023 g of the salt in 60 ml of double-distilled water. About 4 ml of 1.00 mM tetrachloroauric acid aqueous solution was taken in a centrifuge tube of 10 ml capacity. To this, 0.4 ml of the freshly prepared cinnamon extract was added using a glass pipette, and the content mixed using a glass rod. The tube was placed in a microwave oven and heated for 15 min in the microwave oven of 1000 W. The solution turned from light yellow to a purple-red color indicating the formation of colloidal gold nanoparticles.

2.3 Transmission electron microscopy (TEM)

The gold nanoparticle was characterized using FEI Morgagni 268 transmission electron microscope operating at an accelerating voltage of 80 kV. The sample was prepared by depositing a drop of the colloidal nanoparticles on a carbon support grid. The grid was air-dried, and images of the gold nanoparticles were obtained in the bright-field mode.

2.4 UV-Vis spectroscopy

The absorption spectrum of the samples was measured using a double-beam Shimadzu UV-1800 spectrophotometer. The colloidal Au nanoparticle (~2.5 ml) was placed in a cuvette of path length of 1 cm, and the absorption spectrum was recorded in the wavelength range 350-700 nm with 1mm resolution.

2.5 Fourier Transfer Infra-red (FTIR)spectroscopy

The infra-red spectrum of the colloidal gold nanoparticles, Congo red, and the complexes of Congo red with gold ions was collected using a Bruker Alpha spectrophotometer in the scanning range of 500–4000 cm^{-1}. The samples were prepared as solid and transparent pellets with dry potassium bromide (KBr).

III. Results and Discussion

3.1 Formation and characterization of gold nanoparticles

The formation of colloidal gold nanoparticles was confirmed by the change in the color of the solution. The color of the solution changed from light yellow to purple-red color after microwave heating. This along with a characteristic peak surface plasmon resonance (SPR) confirmed the formation of gold nanoparticles from gold salt in aqueous solution. Fig. 1 shows the UV-Vis spectrum of the synthesized gold nanoparticles. The spectrum shows a strong SPR peak at around 536 nm.

The SPR arises from the collective oscillation of electrons on the surface of the gold nanoparticle causes this phenomenon resulting in strong excitation of light (absorption and scattering) [30]. The presence of a single SPR peak indicates that the colloidal gold nanoparticles are poly disperse and are mainly spherical in shape. The peaks wavelength at which this phenomenon occurs is strongly dependent on the physical state of the gold nanoparticle such as size, shape, agglomeration, and aggregation state [30,31].

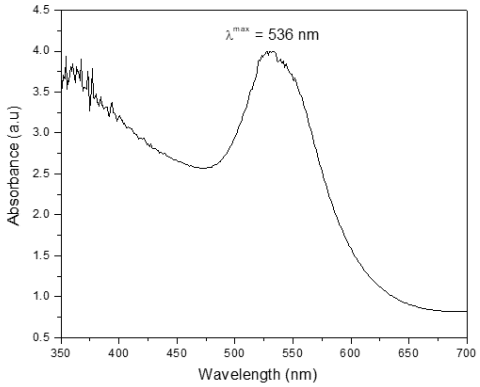

Fig. 1. UV-Vis absorption spectrum of colloidal gold nanoparticles in water.

The size and morphology of the gold nanoparticles were further studied using TEM, and the micrograph is shown in Fig. 2. The gold nanoparticles are spherical and polydisperse (15 %) with an average diameter of 35 nm. Based on the SPR peak (λ^{max}) at 535nm, the size of the gold nanoparticles in solution was estimated to be around 40 nm using a calibration curve of gold nanoparticle size versus optical density [30-34]. This value is quite close the reported value by TEM. The TEM image shown were taken after 1 month, thus these results indicate the successful synthesis of stable gold nanoparticles in aqueous solution by the chemical reduction of $HAuCl_4$with cinnamon extract, and almost with no aggregations.

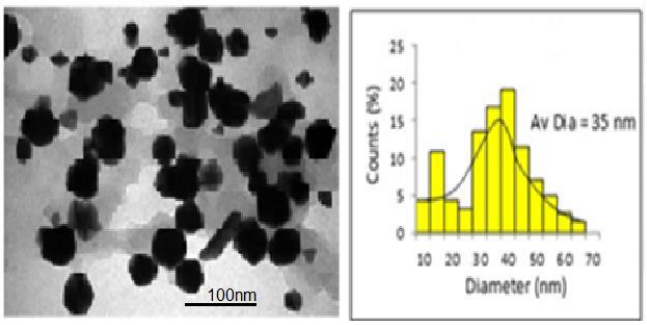

Fig. 2.TEM imageand size histogram of the gold nanoparticles.

The phytochemicals present in cinnamon are 1–4 wt % of essential oils (*trans*-cinnamaldehyde, *trans*-cinnamic acid, eugenol, linalool, terpenes, and others), 5–10wt% of polyphenols (catechin, epicatechin, anthocyanidin, catechin/epicatechin oligomers, kaempferitrin, and 18 others) and 80–90 wt % of carbohydrates (starch, polysaccharides, and ash). These chemical components contain active functional groups such as hydroxyl, aldehyde, and carboxyl that are believed to play a vital role in the chemical reduction of $HAuCl_4$ to gold nanoparticles [27-29]. The chemical structures of the most important phytochemicals of cinnamon that are responsible for chemical reduction of $HAuCl_4$ to gold nanoparticles are shown in Fig. 3.

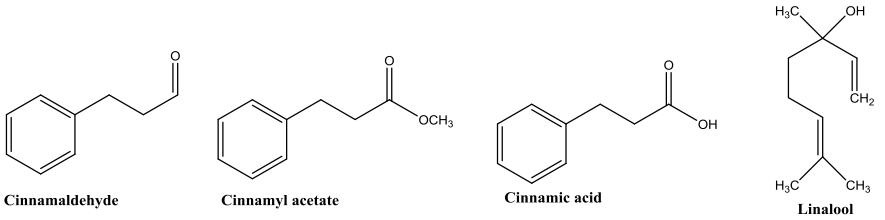

Fig. 3. Chemical structures of some important phytochemicals present in cinnamon.

Among these, the cinnamaldehyde and linalool present in the cocktail of chemicals in thecinnamon extract are the primary reducing agents that reduce Au(III) ions to gold nanoparticles in solution [29,35]. The carbohydrates present in the extract act as stabilizers for the gold nanoparticles against agglomeration. Overall, the cocktail effect of various phytochemicals present in cinnamon provides simultaneous chemical reduction of $HAuCl_4$ and stabilization of gold nanoparticles against agglomeration in aqueous solution. The formation and stabilization of gold nanoparticles from the precursor gold salt using cinnamon extract is illustrated in Fig. 4.

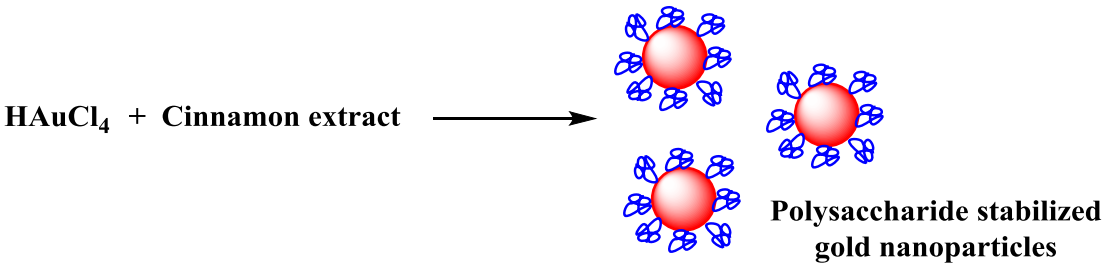

Fig. 4. Illustration of formation of gold nanoparticles from gold salt using cinnamon extract.

3.2 General characteristics of Congo red (CR)

The azo dyes are the largest class of organic dyes that contains azo group (–N=N–) as the chromophore. Congo red with chemical formula $C_{32}H_{22}N_6Na_2O_6S_2$ is a bisazo dye which is readily soluble in water and gives intense red color. The chemical structure of Congo red is given in Fig.5, and the chromophores in the dye are the naphthalene, azo, and phenyl groups [36].

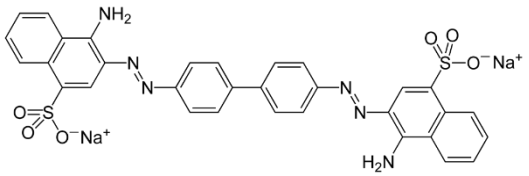

Fig.5. Chemical structure of the dye, Congo red.

3.3 Absorption spectrum of Congo red

The absorption spectrum of the samples at 23 °C is shown in Fig.6.

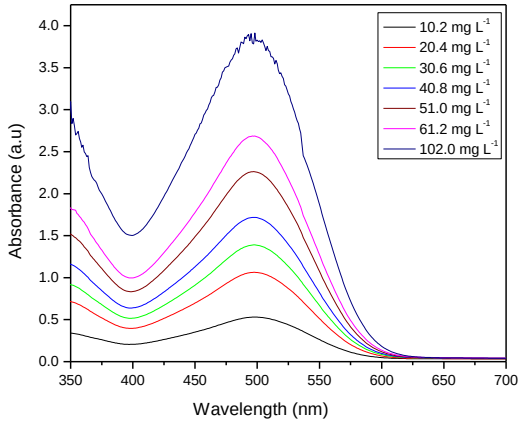

Fig.6. UV-Vis spectra of Congo red aqueous solution at 23 °C (spectra truncated to show only the peak of interest 497 nm).

The spectra of CR showed three distinct absorption peaks at 497 nm ($\pi \rightarrow \pi^*$ transition of azo group), 340 nm ($\pi \rightarrow \pi^*$ transition of NH group), and 235 nm. However, the peak at 497 nm (λ_{max}) is the peak of interest as this is present in the visible region of the spectrum and is responsible for the π-electron transition of the azo groups. With increase in theconcentration of CR, the absorption peak becomes sharp and shows no spectral perturbations. This change in shape (broad to narrow) of the absorption peak is due to the self-aggregation characteristic of CR. During self-aggregation in water, the CR molecules aggregate through π-stacking of the benzene rings leading to the formation of cylindrical or rod-like micelles [37, 38].

3.4 The interaction of Congo red with gold salt (Au^{3+} ions)

To investigate the effect of gold ions on the interaction with Congo red, the concentration of the dye was fixed at 61.2 mg L^{-1} (8.78×10^{-5} M), and the concentration of the gold salt was variedsystematically (9.90×10^{-5} M, 1.96×10^{-4} M, 2.91×10^{-4} M, 3.85×10^{-4} M, 5.86×10^{-4} M and 7.41×10^{-4} M). The change in absorbance of CR aqueous solution with anincreasing concentration of gold salt is shown in Fig.7.

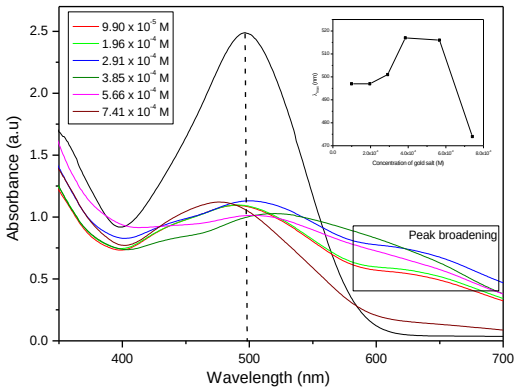

Fig.7. Effect of gold salt on the absorbance of CR aqueous solution, measured at 23 °C.

Upon adding the gold ions in the form of $HAuCl_4$solutions of various concentrations to CR solution, the absorbance of CR decreases significantly. The decrease in absorbance for all the concentrations of gold salt is about 56% ± 6%. In addition to this significant decrease in absorbance, two other major effects are observed viz. (i) theprogressive shift in λ_{max} to longer wavelength (shown as an inset in Figure 8) and (ii) additional broad tail peak at λ = 627 nm. These spectral changes are attributed to coordinate complex formation between CR and Au^{3+} ions through electrostatic interactions. The stoichiometry of the complexation reaction was estimated from a plot of λ_{max} versus the molar ratio of $HAuCl_4$/CR [39]. From the inflection point in the plot, the stoichiometry of the reaction was estimated to be 3 mol of $HAuCl_4$ for 1 mol of CR. Further, the intensity of the new broad

peak at λ = 627 nm increased withanincrease in theconcentration of gold salt, which further confirms the stoichiometry of the complexation reaction.

3.5 Kinetics of interaction of Congo red with gold salt (Au^{3+})

The kinetics of interaction of CR with Au^{3+} ions was also studied by following the time-dependent absorbance for 10 min in intervals of 1 min for a fixed concentration of CR (8.78×10^{-5} M) and $HAuCl_4$ (2.91×10^{-5} M). The change in absorbance as function of time is shown in Fig.8.

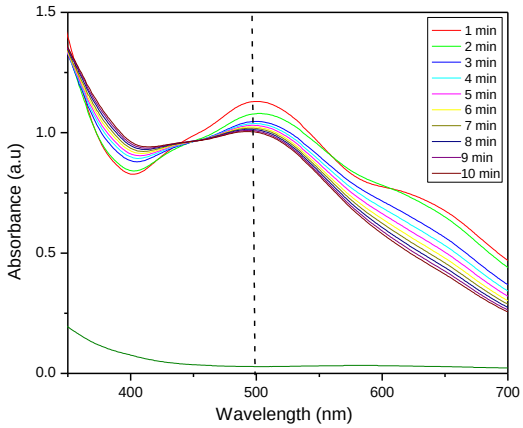

Fig.8. Time-dependent absorbance for acomplex forming reaction between CR and Au^{3+} ions.

The absorbance shows a significant decrease in intensity (~ 55 %) during the first 1 min followed by a gradual decrease for the first 10 min. A new broad peak with asignificant tail is observed at λ = 627 nm. These observations indicate the complex formation reaction between CR and Au^{3+} ions to be slow but gradual during the first 10 min. Interestingly, after 24 h, the absorbance of the solution decreased very significantly to about 0.028, which corresponds to abouta99% decrease in intensity. A pale pink residue was observed at the bottom of the cuvette and the solution was colorless further confirming the formation of the insoluble and aggregated form of CR-Au complexes. The complexes formed self-aggregate in aqueous solutions through various physical interactions such as hydrophobic interactions, π-electron interactions, H-bonding, and dispersion forces [40]. The size of the aggregates depends on the concentration and type of dye. These observations agree with the formation of CR complexes with various proteins [41,42]. The formation of the CR-Au complex and its precipitation from the solution due to aggregation is illustrated in Fig.9.

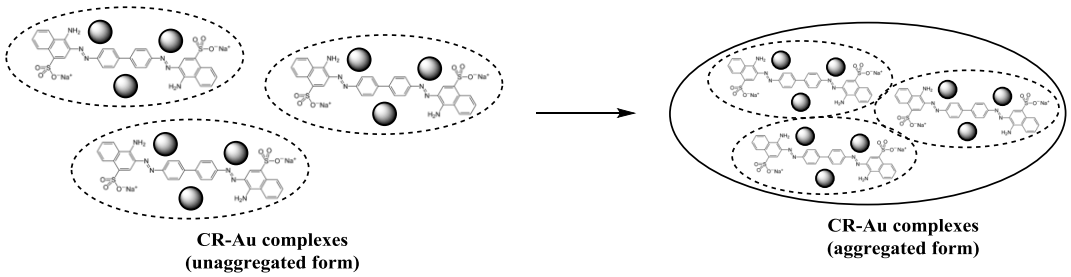

Fig.9. Illustration of unaggregated and aggregated CR-Au^{3+} complexes in aqueous solution.

3.6 Infra-red spectroscopy of CR-Au complex

The formation of CR-Au complex was confirmed using infra-red spectroscopy. The FTIR spectrum of Congo red and the CR-Au complex are shown in Fig.10.

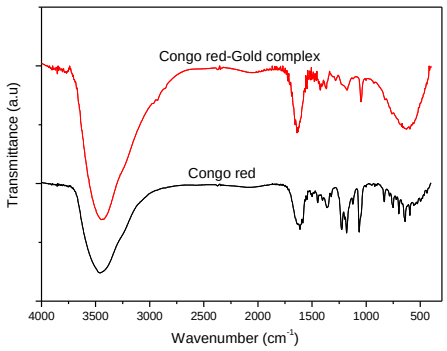

Fig.11. FTIR spectrum of CR and CR-Au complexes as KBr pellet.

For CR, the following characteristic absorption peaks are identified: 1607 cm^{-1} and 1495 cm^{-1} (aromatic rings), 1589 cm^{-1} (–N=N–), 3460 cm^{-1} (-NH_2), and 1196 cm^{-1} (S–O). The IR spectrum of CR-Au complex appears like the pure CR, however distinct peak shifts can be observed. The weak peak of (–N=N–) is shifted from 1589 cm^{-1} to 1641 cm^{-1} and this peak shift indicates that the nitrogen atomis involved in the formation of acomplex with gold ion. Similar peak shifts have been observed for CR complexes with divalent metal ions such as copper, nickel, zinc, and lead [43].

3.7 Interaction of Congo red with gold nanoparticles

The interaction of CR with colloidal gold nanoparticles in aqueous solution is not well documented in the literature. In general, the degradation of CR by metal nanoparticles in the presence of a strong reducing agent such as sodium borohydride ($NaBH_4$) has been well studied. To gain an insight into the nature of theinteraction of CR with gold nanoparticles in the absence of any reducing agents, the absorbance spectra of CR as afunction of the concentration of gold particles was recorded and the result is shown in Fig.11. The absorbance spectrum of the colloidal gold solution is also included in the same figure as reference.

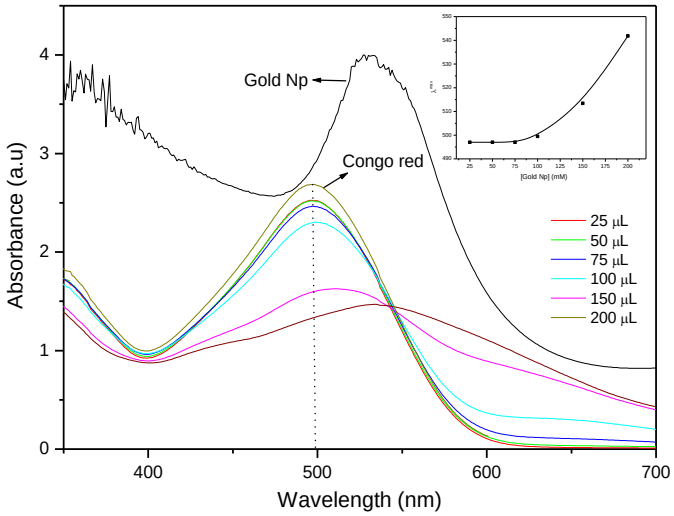

Fig.11. Influence of gold nanoparticles on the absorption of CR solution.

With an increase in concentration (in number) of gold nanoparticles, the absorbance of CR decreases systematically up to a particle concentration of 11.1×10^{10}. When the particle number concentrations are 16.6×10^{10} and 22.2×10^{10}, the absorbance of CR decreases significantly with the shifting of λ^{max} to longer wavelength (redshift). In addition, a new broad shoulder with asignificant tail is observed at thewavelength λ = 627 nm for higher concentrations of gold nanoparticles. As can be seen from Fig.11 the broad shoulder peak increases in intensity with an increase in the concentration of gold nanoparticles in CR aqueous solution. The enhancement in intensity of broader shoulder constituted a proof of interaction between CR and Au nanoparticles. Visual image of congo red solutions containing various amounts of gold nanoparticles is shown in Fig. 12.

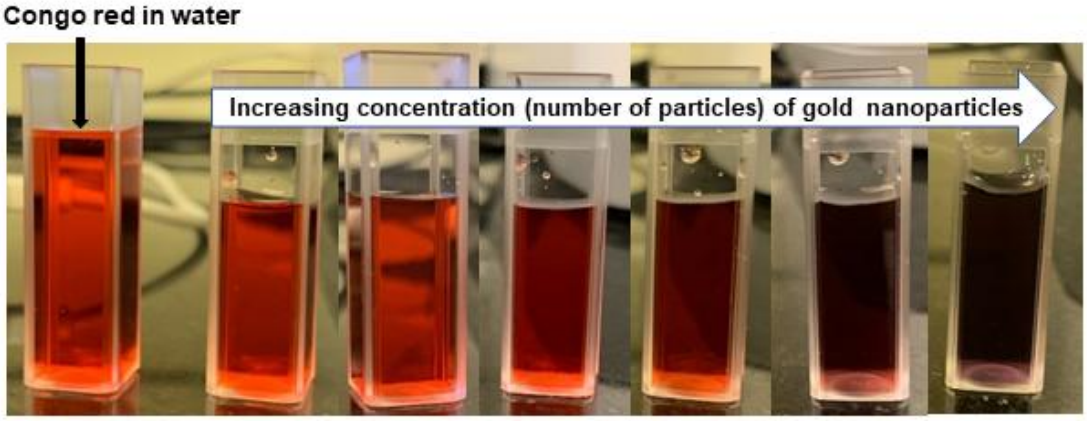

Fig. 12. Visual observation of CR solution as a function of the concentration of gold nanoparticles.

These results unambiguously indicate the formation of stable complexes between CR and colloidal gold nanoparticles in aqueous solution. It is envisaged that the negative sulfonic groups (SO_3^-) of CR adsorbs onto the positively charged surface of gold nanoparticles through strong electrostatic interactions leading to the formation of a stable complex. An illustration of the complex formed between CR and colloidal gold nanoparticles is shown in Fig. 13.

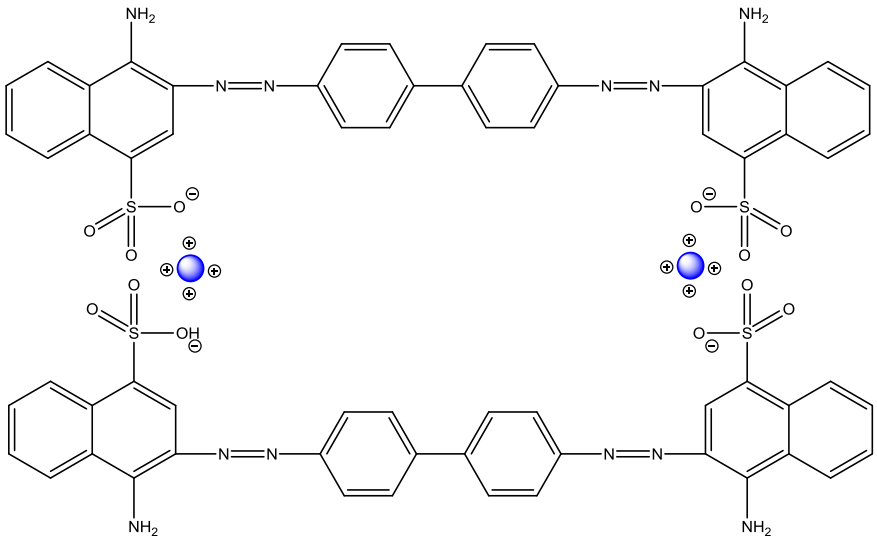

Fig. 13. Illustration of the complex formed between CR and gold nanoparticles in aqueous solution.

Therefore, in the absence of chemical reducing agents such as $NaBH_4$, CR forms a stable complex with metal nanoparticles and is not degraded into any other chemical species. The gold nanoparticles both at low and high concentrations impart stability to the CR-gold nanoparticle complexes through electrostatic interactions. A 3D representation of the complexes at low and high concentrations of gold nanoparticles is illustrated in Fig. 14.

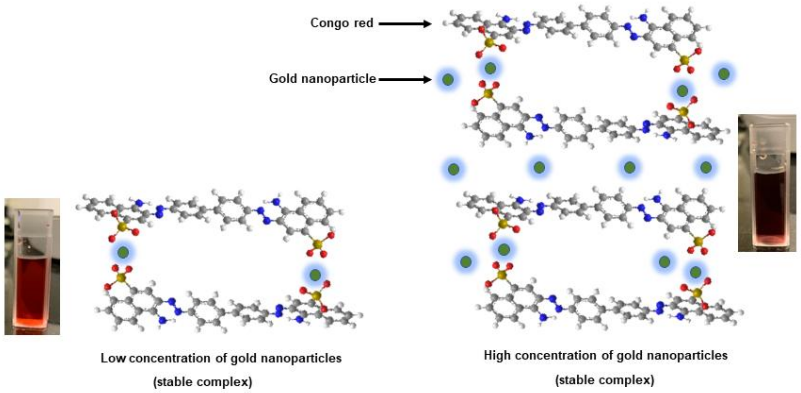

Fig. 14. Three-dimensional representation of complexes formed between CR and gold nanoparticles at low and high concentration in aqueous solution.

The results agree with that reported for the formation of complexes between CR and silver nanoparticles in aqueous solution [44], and with complexes of gold nanoparticles and bovine serum albumin, cytochrome c, and lysozyme [45,46]. In general, CR self-aggregates and forms a stable complex with surfactants, proteins, and macromolecules [47]. Further, the results indicate that CR has a strong complex forming ability with metal salts of silver and gold and their nanoparticles. It must be pointed that chemical degradation of CR takes place only in the presence of metal nanoparticles and a chemical reducing agents viz. $NaBH_4$ and citric acid.

IV. Conclusions

Stable gold nanoparticles with low polydispersity were successfully synthesized by a green method using an extract of cinnamon. The active phytochemicals present in the extract maybe responsible in reducing the Au^{3+} to Au nanoparticles, and the carbohydrates provided stability against agglomeration. The interaction of gold ions (Au^{3+}) and Au nanoparticles with CR were studied in detail using UV-Vis absorption spectroscopy. CR formed a complex with gold ions which aggregated over time and the aggregation process was rather gradual. With gold nanoparticles, CR also formed complex at both low and high concentrations of nanoparticles. The gold nanoparticles offered stability of the complex due to strong electrostatic interactions. Degradation of CR in the presence of gold ions and gold nanoparticles was not observed due to the absence of chemical reducing agents. This study has shown that gold ions and gold nanoparticles are capable of only forming complexes with CRand do not catalytically degrade the dye. For the catalytic degradation to occur, a chemical reducing agent is thus required along with gold nanoparticles to enhance the electron transfer reactions involved during the degradation process.

Acknowledgement

The authors acknowledge the RCSI Summer School for financial support. Ms. Fatima Al Hannan is thanked for her help during the experiment.

Authors Declaration

The authors declare no conflict of interest.

[1]. J.O. Duruibe, M.D.C. Ogwuegbu, J.N. Egwurugwu, Heavy metal pollution and human bio toxic effects, Int. J. Phys. Sci. 2 (2007) 112-118.
[2]. E. Weisburger, Cancer-causing chemicals, In Cancer—The outlaw cell, R.F. LaFond, Ed. American Chemical Society: Washington D.C. (1978) 173-186.
[3]. E.N. Abrahart, Dyes and their intermediates, Chemical publishing: New York, (1977) 1-12.
[4]. R.H. Meade, Contaminants in the Mississippi river, Geological survey circular 1133, Reston, Virginia (1995).
[5]. E. Forgacs, T. Cserhati, G. Oros, Removal of synthetic dyes from wastewater: a review, Environ. Int. 30 (2004) 953-971.
[6]. O. Gercel, H.F. Gercel, A.S. Koparal, U.B. Ogutveren, Removal of disperse dye from aqueous solution by novel adsorbent prepared from biomass plant material, J. Hazard Mater. 160 (2008) 668-674.
[7]. N. Amin, Removal of direct blue-106 dye from aqueous solution using new activated carbons developed from pomegranate peel: adsorption equilibrium and kinetics, J. Hazard Mater. 165 (2009) 52-62.
[8]. S. Deng, Y. Peng-Ting, Polyethyleneimine-modified fungal biomass as a high capacity biosorbent for Cr(VI) anions: sorption capacity and uptake mechanisms, Envir. Sci. Tech. 39 (2005) 8490-8496.
[9]. V.V. Panic, Z.P. Madzarevice, T. Volkov-Husovic, S.J. Velickovic, Poly(methacrylic acid) based hydrogels as sorbents for removal of cationic dye basic yellow 28: kinetics, equilibrium study and image analysis, Chem. Eng. J. 217 (2013) 192-204.
[10]. T. Robinson, G. McMullan, R. Marchant, P. Nigam, Remediation of dyes in textile effluent: a critical review on current treatment technologies with a proposed alternative, Biores. Technol. 77 (2001) 247-255.

[11]. N. Masoudzadeha, F. Zakeria, T.B. Lotfabada, H. Sharafi, F. Masoomi, H.S. Zahiri, G. Ahmadian, K.A. Noghabi, Biosorption of cadmium by Brevundimonassp. ZF12 strain, a novel biosorbent isolated from hot-spring waters in high background radiation areas, J. Hazard Mater. 197 (2011) 190-198.

[12]. S. Song, A. Lopez-Valdiviesco, D.J. Hernandez-Campus, C. Peng, M.G.Montoy-Fernandez, I. Razo-Soto, Arsenic removal from high arsenic water by enhanced coagulation with ferric ions and coarse calcite, Water Res. 40 (2006) 364-372.

[13]. H. Dong, X. Guan, D. Wang, C. Li, X. Yang, X. Dou, A novel application of H2O2-Fe(II) process for arsenate removal from synthetic acid mine drainage (AMD) water, Chemosphere 85 (2011) 1115-1121.

[14]. E. Dana, A. Sayari, Adsorption of heavy metals on amine-functionalized SBA-15 prepared by co-condensation: applications to real water samples, Desalination 285 (2012) 62-67.

[15]. G. Roshan Deen, Stimuli-responsive cationic polymers for biomedical applications, In Encyclopedia of Biomedical Polymers and Polymeric Biomaterials, M. Mishra, Ed., Taylor and Francis: New York, USA (2015) 1334-1343.

[16]. B. Reddy, G.M. Alle, R. Dadigala, R. Dasari, V. Maragoni, V. Guttena, Catalytic reduction of methylene blue and Congo red dyes using green synthesized gold nanoparticles capped by salmaliamalabarica gum, Int. Nano Lett. 5 (2015) 215-222.

[17]. S. Ashokkumar, S. Ravi, V. Kathiravan, S. Velmurugan, Synthesis, characterization and catalytic activity of silver nanoparticles using Tribulus terrestris leaf extract, Spectrochim. Acta Part A. Mol. Biol. Spectros. 121 (2014) 88-93.

[18]. B. Cheng, Y. Le, W. Cai, J. Yu, Synthesis of hierarchical $Ni(OH)_2$ and NiO nanosheets and their adsorption kinetics and isotherms to Congo red in water, J. Hazard Mater. 185 (2011) 889-897.

[19]. X. Liang, L. Zhao, Room-temperature synthesis of air-stable cobalt nanoparticles and their highly efficient adsorption ability of Congo red, RSC Adv. 2 (2012) 5485-5487.

[20]. S.K. Hashimi, G.J. Hutchings, Gold catalysis, Angew. Chem. Int. Ed. Engl. 45 (2006) 7896-7936.

[21]. A. Kumar, X. Zhang, X. Liang, Gold nanoparticles: emerging paradigm for targeted drug delivery system, Biotechnol. Adv. 31 (2013) 593-606.

[22]. K. Sneha, M. Sathish Kumar, S.Y. Lee, M.A. Bae, Y-S. Sun, Biosynthesis of Au Nanoparticles using cumin seed powder extract, J. Nanosci. Nanotech. 11 (2011) 1811-1814.

[23]. B. Sharma, R. Deswal, Single pot synthesized gold nanoparticles using Hippophae rhamnoides leaf and berry extract showed shape-dependent differential nanobiotechnological applications, Artif. Cells Nanomed. Biotechnol. 46 (2018) 408- 418.

[24]. F.S. Roasarin, S. Mirunalini, Nobel metallic nanoparticles with novel biomedical properties, J. Bioanal. Biomed. 03 (2011) 85-91.

[25]. C. Umamaheswari, A. Lakshmanan, N.S. Nagarajan, Green synthesis, characterization, and catalytic degradation studies of gold nanoparticles against Congo red and methyl orange, J. Photochem. Photobiol. B: Biol. 178 (2018) 33-39.

[26]. C.F. Mao, M.C. Hsu, W.H. Hwang, Physicochemical characterization of grifolan: thixotropic properties and complex formation with Congo red, Carbohyd. Polym. 68 (2007) 502-510.

[27]. S. Mathew, T.E. Abraham, Studies on the antioxidant activities of cinnamon (Cinnamomum verum) bark extracts through various in vitro models, Food Chem. 94 (2006) 520-528.

[28]. P. Lopez, C. Sanchez, R. Batlle, C. Nerin, Vapor-phase activities of cinnamon, thyme and oregano essential oils and key constituents against foodborne microorganism, J. Agri. Food Chem. 55 (2007) 4348-4356.

[29]. R. Kannan, V. Rahing, C. Cutler, R. Pandrapragada, K.K. Katti, V. Kattumuri, J.D. Robertson, S.J. Casteel, S. Jurisson, C. Smith, E. Boote, K.V. Katti, Nanocompatible chemistry toward fabrication of target-specific gold nanoparticles, J. Am. Chem. Soc. 128 (2006) 11342-11343.

[30]. Y. Sun, Y. Xia, Gold and silver nanoparticles, Analyst 128 (2003) 686-691.

[31]. J. M. Slocik, J.S. Zabinski Jr, D.M. Phillips, R.R. Naik, Colorimetric response of peptide-functionalized gold nanoparticles to metal ions, Small 4 (2008) 548-551.

[32]. M.J. Cavaluzzi, P.N. Borer, Revised uv extinction coefficients for nucleoside-5'-monophosphates and unpaired DNA and RNA, Nucleic Acids Res. 32 (2004) 13-16.

[33]. W. Haiss, N.K.T. Thanh, J. Aveyard, D.G. Fernig, Determination of size and concentration of gold nanoparticles from uv-vis spectra, Anal. Chem. 79 (2007) 4215-4221.

[34]. S. Rahman, Size and concentration analysis of gold nanoparticles with ultraviolet-visible spectroscopy, Undergrad. J. Mathem. Model. 7 (2016) 1-13.

[35]. J. Usta, S. Kreudiyyeh, P. Barnabe, Y. Bou-Moughlabay, H. Nakkash-Chmaisse, Comparative study on the effect of cinnamon and clove extracts and their main components on different types of ATPases, Hum. Exp. Toxicol. 22 (200) 355-362.

[36]. M. Giri, N. Jaggi, N. Singh, R.M.P. Jaiswal, Absorption, excitation and fluorescence spectra of Congo red in aqueous solutions, Indian J. Phys. 78 (2004) 1137-1140.

[37]. W.G. Turnell, J.T. Finch, Binding of the dye Congo red to the amyloid proteins pig insulin reveals novel homology amongst amyloid-forming peptide sequences, J. Mol. Biol. 227 (1992) 1205-1223.

[38]. R. Chang, Physical Chemistry for the Biosciences. USA: University Science Books, (2005).

[39]. R.T. Tarawneh, I.I. Hamdan, A. Bani-Jaber. R.M. Darwish, Physicochemical studies on Ciclopirox olamine complexes with divalent metal ions, Int. J. Pharm. 289 (2005) 179-187.

[40]. M. Skovronek, B.Stopa, L. Konieczny, J. Rybarska, B. Piekarska, E. Szneler, G. Bakalarski, I.Roterman, Self-assembly of Congo red—a theoretical and experimental approach to identify its supramolecular aggregation in water and salt solutions, Biopolymers 46 (1998) 267-281.

[41]. K. Yokoyama, A.D. Fisher, A.R. Amori, D.R. Welchons, R.E. McKnight, Spectroscopic and calorimetric studies of Congo red dye-amyloid β peptide complexes, J. Biophys. Chem. 1 (2010) 153-163.

[42]. J. Sereikaite, V.A. Bumelis, Congo red interactions with α-proteins, Acta Biochim. Pol. 53 (2006) 87-91.

[43]. M. Jayandran, Cyclic voltammetric and ultrasonic technique on disodium 4-amino-sulfonate dye with Cu, Ni, Zn and Pb complexes, Int. J. British 1 (2014) 44-52.

[44]. S.A. Al-Thabaiti, E. S. Aazam, Z. Khan, O. Bashir, Aggregation of Congo red with surfactants and Ag-nanoparticles in an aqueous solution, Spectrochim. Acta Part A: Mol. Biomol. Spect. 156 (2016) 28-35.

[45]. A. Mahal, M.K. Goshisht, P. Khullar, H. Kumar, N. Singh, G. Kaur, M.S. Bakshi, Protein mixtures of environmentally friendly zein to understand protein-protein interactions through biomaterial synthesis, hemolysis, and their antimicrobial activities, Phys. Chem. Chem. Phys. 16 (2014) 14257-14270.

[46]. M.KGoshisht, L. Moudgil, M. Rani, P. Khullar, G. Singh, H. Kumar, N. Singh, G. Kaur, M.S. Bakshi, Lysozyme complexes for the synthesis of functionalized biomaterials to understand protein-protein interactions and their biological applications, J. Phys. Chem. C 118 (2014) 28207-28219.

[47]. B.R. Craven, A. Datyner, The interaction between some acid wool dyes and nonylphenol -ethylene oxide derivatives, J. Soc. Dye Colour. 79 (1963) 515-519.